Journal of Multidisciplinary Engineering Science and Technology (JMEST)
ISSN: 2458-9403
Vol. 3 Issue 5, May - 2016

On The Performance Of Sensorless Vector Controlled Induction Motor Drives With Parallel Stator Resistance And Rotor Speed Estimation

Ahmed Kh. Taha [1], Mahmoud A. Elwany[2] and Barakat M. Hassaneen [1]

[1]Depart. of Electrical Engineering, Faculty of Engineering, Alazhar University, Qena, Egypt
[2] Depart. of Electrical Engineering, Faculty of Engineering, Alazhar University, Cairo, Egypt

***Abstract*—The main goal of this paper is to provide a novel method of parallel stator resistance and rotor speed estimation for sensorless indirect field oriented controlled induction motor drive. In this scheme, a parallel model reference adaptive system (MRAS) is designed to simultaneous estimation of rotor speed and stator resistance in order to achieve high-precise control in a wide range of motor speed. Moreover, the stability of the control scheme has been derived based on Popov's criterion. Matlab/Simulink software has been carried out in order to evaluate the effectiveness of the proposed scheme at different operating conditions. The results demonstrate the activity of the scheme at wide range speed operation with load disturbance and parameters variation.**

Keywords—Model Reference Adaptive System, MRAS, Induction Motor, Indirect field oriented control, Vector control. Speed Estimation, Stator Resistance Estimation.

I. Introduction

High performance electric motor drives are considered an essential requirement for modern industrial applications. In the past, dc motors have been widely used for this purpose. However, heavy weight, large size and frequent maintenance requirements make dc motors an expensive solution. In addition to undesired sparking resulting from the mechanical commutator-brush. These inherent drawbacks of dc motors have prompted continual attempts to find out a better solution for the problem.so induction motors are widely used as variable speed drives in industries due to their advantages like rugged construction, low cost, low maintenance and better performance [1]. Torque and speed control of an induction motor is now possible due to the recent developments in power electronics and digital signal processors (DSP) using field oriented control technique. There are two general methods of field oriented control. The direct method and the indirect method. The direct field oriented control method depends on generating unit vector signals, required for flux orientation, from the fluxes measured using Hall-effect flux sensors or search coils, or estimated. The indirect field oriented method uses the rotor speed and the slip angular frequency derived from the rotor dynamic equations to generate the unit vector signals to achieve flux orientation. Although Indirect field orientation method is very sensitive to variations of motor parameters [2]. This paper is aimed at developing a method of speed sensorless vector-control of induction motor drive system. A model reference adaptive system is one of the important techniques that used to estimate the speed for speed sensorless induction motor drives, because it is simple and easy to implement and take minimum processor time [3]. However, it exhibit lower accuracy due to parameter variation [4]. The accuracy of speed estimator is strongly affected by stator resistance variation especially at low speed range of operation [5]. In this paper, to overcome the problem of operation in low speed range a modified MRAS will be used to estimate the motor speed and stator resistance simultaneously from measured stator voltages and currents. Moreover, in this scheme, the structure of the estimator is modified in such a way that the variation of stator resistance and load torque is recognized within the speed and stator resistance estimation algorithm. A digital simulation is carried-out for speed sensorless indirect vector controlled induction motor drives to investigate how the system performance is influenced by stator resistance variation which vary by temperature variation. To validate the effectiveness and accuracy of the proposed simulation algorithm, the calculated motor speed, stator current, rotor flux components and motor torque are investigated.

List of symbols

V_{ds}, V_{qs} The *d*-q axis stator voltage components (V)

i_{ds}, i_{qs} The *d*-q axes stator current components (A)

i_{ds}^*, i_{qs}^* The *d*-q axes desired stator currents components (A)

i_{dr}, i_{qr} The *d*-q axes rotor current components (A)

i_{ds}^s, i_{qs}^s Stationary axes stator current components (A)

i_{dr}^{s}, i_{qr}^{s} Stationary axes rotor current components (A)

L_m Magnetizing inductance (H)

$\hat{L}_m$ Estimated Magnetizing inductance (H)

L_r Rotor self-leakage inductance (H)

L_s Stator self-leakage inductance (H)

L_{ls} , L_{lr} Stator and Rotor leakage inductance (H)

σ Leakage coefficient $\left(1 - L_m^2 / L_s L_r\right)$

T_l , T_e Load and Electromagnetic torques (Nm)

R_s , R_r Stator and Rotor resistances (Ω)

$\hat{R}_r$ Estimated rotor resistance (Ω)

ω_e Synchronous speed (rad/sec)

ω_e^* Command synchronous speed (rad/sec)

ω_{sl} Slip speed (rad/sec)

ω_{sl}^* Command slip speed (rad/sec)

ω_r , ω_r^* Actual and Reference Rotor speed (rad/sec)

$\hat{\omega}_r$ Estimated Rotor speed (rad/sec)

θ_e Angle between synchronous frame and stationary frame

T_r Rotor time constant $T_r = L_r / R_r$

f_d The damping coefficient of the load

J Moment of inertia (kg.m^2)

$\lambda_{dr}^{s}, \lambda_{qr}^{s}$ Stationary axes rotor flux components (wb)

$\hat{\lambda}_{dr}^{s}, \hat{\lambda}_{qr}^{s}$ Stationary axes estimated rotor flux components (wb)

$\vec{\lambda}_r$ Rotor flux vector (wb)

λ_{dr} , λ_{qr} The d-q axes rotor flux components (wb)

$p = d/dt$ Differential operator

p No of poles

II. Dynamic Model of Induction Motor

The dynamic model of the IM is modified from the traditional model of a three phase, Y-connected induction motor in $d^s - q^s$ stationary reference frame and can be described by the following differential equations [15]:

$$\frac{di_{qs}^{s}}{dt} = -\left(\frac{R_s}{L_s\delta} + \frac{R_r L_m^2}{L_s L_r^2 \delta}\right) i_{qs}^{s} + \frac{R_r L_m}{L_s L_r^2 \delta} \lambda_{qr}^{s} - \frac{L_m}{L_s L_r \delta} \omega_r \lambda_{dr}^{s} + \frac{1}{L_s \delta} V_{qs}^{s} \quad (1)$$

$$\frac{di_{ds}^{s}}{dt} = -\left(\frac{R_s}{L_s\delta} + \frac{R_r L_m^2}{L_s L_r^2 \delta}\right) i_{ds}^{s} + \frac{L_m}{L_s L_r \delta} \omega_r \lambda_{qr}^{s} + \frac{R_r L_m}{L_s L_r^2 \delta} \lambda_{dr}^{s} + \frac{1}{L_s \delta} V_{ds}^{s} \quad (2)$$

$$\frac{d\lambda_{qr}^{s}}{dt} = \frac{R_r L_m}{L_r} i_{qs}^{s} - \frac{R_r}{L_r} \lambda_{qr}^{s} + \omega_r \lambda_{dr}^{s} \quad (3)$$

$$\frac{d\lambda_{dr}^{s}}{dt} = \frac{R_r L_m}{L_r} i_{ds}^{s} - \omega_r \lambda_{qr}^{s} - \frac{R_r}{L_r} \lambda_{dr}^{s} \quad (4)$$

$$\frac{d\omega_r}{dt} = \frac{1}{J}\left(T_e - T_l\right) - \frac{f_b}{J} \omega_r \quad (5)$$

III. Indirect Vector Control of the Induction Motor

The estimation of rotor flux value and its phase angle is performed in rotor flux oriented $d - q$ synchronously rotating reference frame based on stator currents and speed measurement. The condition $\lambda_{qr} = 0$ is satisfied, the influence of q-axis magnetizing flux on resultant magnetizing flux can be neglected ($\lambda_{qm} = 0$).

Simplified indirect vector controller can be described with the following equations:

$$\omega_{sl} = \omega_e - \omega_r \quad (6)$$

And aligning the rotor flux phasor λ_r on the d-axis, the following equations are obtained

$$\lambda_{dr} = \lambda_r \quad (7)$$

$$\lambda_{qr} = 0 = \lambda_{qr} \quad (8)$$

Then the induction motor rotor equations are expressed as;

$$R_r i_{dr} + p\lambda_r = 0 \quad (9)$$

$$R_r i_{qr} + \omega_{sl} \lambda_r = 0 \quad (10)$$

$$i_{qr} = -\frac{L_m}{L_r} i_{qs} \quad (11)$$

$$i_{qr} = \frac{\lambda_r}{L_r} - \frac{L_m}{L_r} i_{ds} \quad (12)$$

and

$$\omega_{sl} = \frac{L_m}{T_r} \frac{i_{qs}}{\lambda_r} \quad (13)$$

$$p\lambda_r = \frac{1}{T_r}\left(-\lambda_r + L_m i_{ds}\right)$$

(14)

$$T_e = K_T i_{qs} \lambda_r \quad (15)$$

where $K_T = \frac{3}{2}\frac{p}{2}\frac{L_m}{L_r} =$ torque constant

Define the command torque- and flux-producing current components i^*_{qs} and i^*_{ds} and using them for the command value of the rotor flux λ^*_r and torque T^*_e

$$i^*_{qs} = \frac{1}{K_T}\frac{T^*_e}{\lambda^*_r} \quad (16)$$

$$i^*_{ds} = \frac{1}{L_m}(1+T_r p)\lambda^*_r \quad (17)$$

The slip speed command ω^*_{sl} is expressed in terms of the command values of rotor flux and torque–producing current component as:

$$\omega^*_{sl} = \frac{L_m}{T_r}\frac{i^*_{qs}}{\lambda^*_r} \quad (18)$$

$$\theta^*_e = \int(\omega_r + \omega^*_{sl})dt \quad (19)$$

IV. Simultaneous Estimation of Stator Resistance and Motor Speed Based on a Modified MRAS

Many schemes based on simplified motor models have been devised to sense the speed of the induction motor from measured terminal quantities for control purposes [6]. The MRAS technique of a sensorless induction motor is highly used to estimate the motor speed because it is simple to implement and uses minimum processor time and memory. However, its accuracy depends on the accuracy of the motor model parameters. Accurate knowledge of stator resistance is not required in indirect field oriented control scheme. However, the speed estimation from the machine terminals quantities depends on the machine model. The disadvantages of this method are that the stator resistance R_s detuning causes motor speed ω_r and torque response deterioration in the low speed range [7]. The basic MRAS motor speed estimator described in [3] and illustrated in Fig.1, where the reference model and adjustable model blocks perform integration of equations (20) and (21). It relies on measured stator currents and measured stator voltages and is composed of the reference (voltage) and the adjustable (current) model. The estimator operates in the stationary reference frame and it is described with the following equations [8]:

$$p\hat{\underline{\lambda}}^s_{rV} = \frac{L_r}{L_m}[\underline{V}^s_s - (\hat{R}_s + \sigma L_s p)\underline{i}^s_s] \quad (20)$$

$$p\hat{\underline{\lambda}}^s_{rI} = \frac{L_m}{T_r}\underline{i}^s_s - \left(\frac{1}{T_r} - j\hat{\omega}_r\right)\hat{\underline{\lambda}}^s_{rI} \quad (21)$$

$$\hat{\omega}_r = \left(K_{p\omega} + \frac{K_{I\omega}}{p}\right)e_\omega \quad (22)$$

$$e_\omega = \hat{\underline{\lambda}}^s_{rI} \times \hat{\underline{\lambda}}^s_{rV} = \hat{\lambda}^s_{drI}\hat{\lambda}^s_{qrV} - \hat{\lambda}^s_{qrI}\hat{\lambda}^s_{drV} \quad (23)$$

where

$\hat{\underline{\lambda}}^s_{rI} = \left[\hat{\lambda}^s_{drI} \quad \hat{\lambda}^s_{qrI}\right]^T$,

$\hat{\underline{\lambda}}^s_{rV} = \left[\hat{\lambda}^s_{drV} \quad \hat{\lambda}^s_{qrV}\right]^T$ and $\underline{i}^s_s = \left[i^s_{ds} \quad i^s_{qs}\right]^T$. A hat above a symbol in equations (20)–(23) denotes estimated quantities, All of the parameters in the motor and the estimator are assumed to be of the same value, except for the stator resistance [hence, a hat above the symbol in equation (20)]. The accuracy of estimated speed depends on the fluxes $\underline{\lambda}^s_{rV}$ derived from stator model of the induction motor. This flux estimation is dependent on the stator resistance R_s of the induction motor as shown by equation (20). At low speeds, the low voltages and variations in the stator resistance due to temperature rise and switch voltage drops and dead times tend to reduce the accuracy of the estimated signals. The error in $\underline{\lambda}^s_{rV}$ estimation due to variation in R_s is known to introduce significant error in speed estimation for speed sensorless drive. These provide the incentive stator resistance R_s estimation [8]. As it is evident from equations (20)–(23) and Fig.1, the adaptive mechanism (PI controller) relies on an error quantity that represents the difference between the instantaneous positions of the two rotor flux estimates. The second degree of freedom, the difference in amplitudes of the two rotor flux estimates, is not utilized. The parallel rotor speed and stator resistance MRAS estimation scheme will make use of this second degree of freedom to achieve simultaneous estimation of the two quantities. The role of the reference and the adjustable model will be interchanged for this purpose, since the rotor flux estimate of equation (21) is independent of stator resistance.

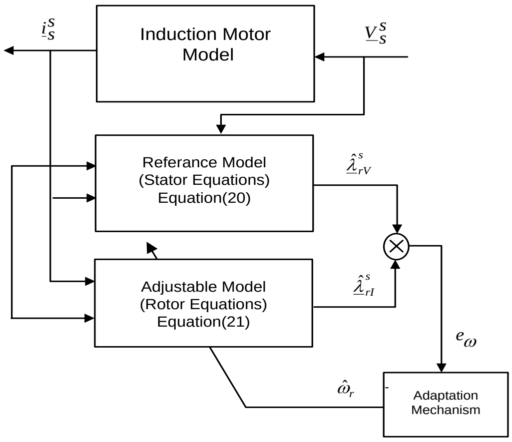

Fig.1: Basic configuration of saturated MRAS speed estimation

Parallel motor speed and stator resistance estimation scheme is designed based on the concept of hyperstability [3] in order to make the system asymptotically stable. For the purpose of deriving an adaptation mechanism, it is valid to initially treat rotor speed as a constant parameter, since it changes slowly compared to the change in rotor flux. The stator resistance of the motor varies with temperature, but variations are slow so that it can be treated as a constant parameter, too. The configuration of the proposed parallel rotor speed and stator resistance is shown in Fig.2.

Let R_s and ω_r denote the true values of the motor stator resistance and rotor speed, respectively. These are in general different from the estimated values. Consequently, a mismatch between the estimated and true rotor flux space vectors appears as well. The error equations for the voltage and the current model outputs can then be written as:

$$p\underline{\varepsilon}_V = -\frac{L_r}{L_m}(R_s - \hat{R}_s)\underline{i}_s^s$$

$$\underline{\varepsilon}_V = \underline{\lambda}_{rV}^s - \hat{\underline{\lambda}}_{rV}^s = \varepsilon_{dV} + j\,\varepsilon_{qV} \tag{24}$$

$$p\underline{\varepsilon}_I = (j\omega_r - \frac{1}{T_r})\underline{\varepsilon}_I + j(\omega_r - \hat{\omega}_r)\hat{\underline{\lambda}}_{rI}^s$$

$$\underline{\varepsilon}_I = \underline{\lambda}_{rI}^s - \hat{\underline{\lambda}}_{rI}^s = \varepsilon_{dI} + j\,\varepsilon_{qI} \tag{25}$$

Symbols $\underline{\lambda}_{rV}^s$, $\underline{\lambda}_{rI}^s$ in the above equations stand for true values of the two rotor flux space vectors. Equations (24), (25) can be rewritten in matrix notation as

$$p\begin{bmatrix}\varepsilon_{dI}\\ \varepsilon_{qI}\\ \varepsilon_{dV}\\ \varepsilon_{qV}\end{bmatrix} = \begin{bmatrix}-\frac{L_r}{R_r} & -\omega_r & 0 & 0\\ \omega_r & -\frac{L_r}{R_r} & 0 & 0\\ 0 & 0 & 0 & 0\\ 0 & 0 & 0 & 0\end{bmatrix}.\begin{bmatrix}\varepsilon_{dI}\\ \varepsilon_{qI}\\ \varepsilon_{dV}\\ \varepsilon_{qV}\end{bmatrix} - W = A\underline{\varepsilon} - W \tag{26}$$

where

$$\underline{\varepsilon}^T = \begin{bmatrix}\varepsilon_{dI} & \varepsilon_{qI} & \varepsilon_{dV} & \varepsilon_{qV}\end{bmatrix} = \begin{bmatrix}\underline{\varepsilon}_I^T & \underline{\varepsilon}_V^T\end{bmatrix}$$

and W is the nonlinear block, defined as follows:

$$W = \left[\begin{array}{c|c} -\Delta\omega_r\begin{bmatrix}0 & -1\\ 1 & 0\end{bmatrix} & \begin{matrix}0 & 0\\ 0 & 0\end{matrix} \\ \hline \begin{matrix}0 & 0\\ 0 & 0\end{matrix} & -\frac{L_r}{L_m}\Delta R_s\begin{bmatrix}1 & 0\\ 0 & 1\end{bmatrix}\end{array}\right].\begin{bmatrix}\hat{\lambda}_{drI}^s\\ \hat{\lambda}_{qrI}^s\\ i_{ds}^s\\ i_{qs}^s\end{bmatrix}$$

$$W = \left[\begin{array}{c|c} -\Delta\omega_r\,\mathrm{J} & 0 \\ \hline 0 & -\frac{L_r}{L_m}\Delta R_s\,\mathrm{I}\end{array}\right].\begin{bmatrix}\hat{\underline{\lambda}}_{rI}^s\\ \underline{\mathrm{i}}_s^s\end{bmatrix}$$

(27) where

$$\Delta\omega_r = \omega_r - \hat{\omega}_r\,,\ \Delta R_s = R_s - \hat{R}_s\,,$$

$$\mathrm{J} = \begin{bmatrix}0 & -1\\ 1 & 0\end{bmatrix},\ \mathrm{I} = \begin{bmatrix}1 & 0\\ 0 & 1\end{bmatrix}$$

The system is hyperstable if the input and output of the nonlinear block W satisfies Popov's criterion [5]

$$s = \int_0^{t_1}\underline{\varepsilon}^T.W\,dt$$

$$= -\int_0^{t_1}\Delta\omega_r\,(\underline{\varepsilon}_I^T.\mathrm{J}.\hat{\underline{\lambda}}_{rI}^s)\,dt + \frac{L_r}{L_m}\int_0^{t_1}\Delta R_s(\underline{\varepsilon}_V^T.\underline{i}_s^s)\,dt$$

$$= S_1 + \frac{L_r}{L_m}S_2 \geq -\gamma^2 \tag{28}$$

$$\underline{\varepsilon}^T.W = -\Delta\omega_r\,(\underline{\varepsilon}_I^T.\mathrm{J}.\hat{\underline{\lambda}}_{rI}^s) + \frac{L_r}{L_m}\Delta R_s(\underline{\varepsilon}_V^T.\underline{i}_s^s)$$

(29)

The validity of equation (28) can be verified using inequality equations (30), (31) with adaptive mechanisms equations (32), (33) for rotor speed estimation and stator resistance identification, respectively:

$$S_1 = -\int_0^{t_1} \Delta\omega_r \,(\underline{\varepsilon}_I^T .\mathrm{J}. \hat{\underline{\lambda}}_{rI}^s)\, dt \geq -\gamma_1^2 \quad (30)$$

$$S_2 = \frac{L_r}{L_m}\int_0^{t_1} \Delta R_s (\underline{\varepsilon}_V^T .\underline{i}_s^s)\, dt \geq \gamma_2^2 \quad (31)$$

$$\hat{\omega}_r = \left(K_{p\omega} + \frac{K_{I\omega}}{p}\right)(\underline{\varepsilon}_I^T .\mathrm{J}. \hat{\underline{\lambda}}_{rI}^s)$$

$$= \left(K_{p\omega} + \frac{K_{I\omega}}{p}\right)(\hat{\underline{\lambda}}_{rI}^s \times \hat{\underline{\lambda}}_{rV}^s)$$

$$\hat{\omega}_r = \left(K_{p\omega} + \frac{K_{I\omega}}{p}\right) e_\omega$$

(32)

where $e_\omega = \hat{\lambda}_{drI}^s \hat{\lambda}_{qrV}^s - \hat{\lambda}_{qrI}^s \hat{\lambda}_{drV}^s$

$$\hat{R}_s = \left(K_{pR_s} + \frac{K_{IR_s}}{p}\right)(-\underline{\varepsilon}_V^T .\underline{i}_s^s)$$

$$= \left(K_{pR_s} + \frac{K_{IR_s}}{p}\right)\left[\underline{i}_s^s \bullet \left(\hat{\underline{\lambda}}_{rV}^s - \hat{\underline{\lambda}}_{rI}^s\right)\right]$$

$$\hat{R}_s = \left(K_{pR_s} + \frac{K_{IR_s}}{p}\right) e_{Rs}$$

(33)

where

$$e_{Rs} = \hat{i}_{ds}^s (\hat{\lambda}_{drV}^s - \hat{\lambda}_{drI}^s) + i_{qs}^s (\hat{\lambda}_{qrV}^s - \hat{\lambda}_{qrI}^s)$$

where $K_{p\omega}$, $K_{I\omega}$, K_{pR_s} and K_{IR_s} are PI parameters of motor speed and stator resistance adaptation mechanisms. The speed and stator resistance can be estimated by equation (31) and equation (32) parallel at any ω. The adaptation mechanism equation (31) is the same as in customary MRAS speed estimator, having only the speed estimation mechanism equation (23).

V. Proposed Sensorless Vector Controlled Induction Motor Drive

Fig .3 shows the block diagram of the proposed sensorless indirect vector controlled induction motor drive. It consists mainly of a loaded induction motor model, a hysteresis current-controlled PWM (CCPWM) inverter, a vector control scheme followed by a coordinate transformation (CT) and an outer speed loop. In addition to the machine and inverter the system include speed controller, an adaptive motor speed estimator. Speed estimator depends on the MRAS technique. The speed controller generates the command q^e – components of stator current $i_{qs}^{*\,e}$ from the speed error between the command speed and the estimated motor speed. The rotor flux reference decreases in inverse proportion to the speed of rotation in the field weakening region, while it is constant and equal to rated rotor flux λ_{rn} in the base speed region.

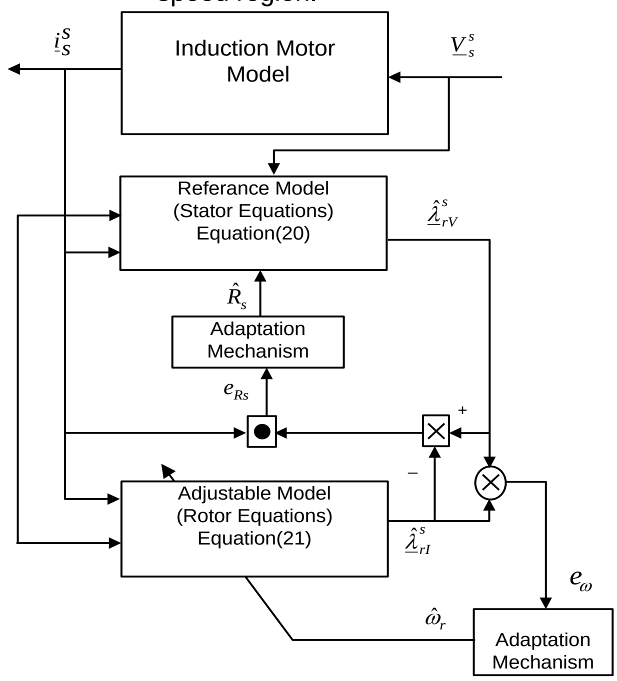

Fig.2: Structure of saturated MRAS system for parallel rotor speed and stator resistance estimation.

As the performance of the MRAS speed estimator is greatly affected by the thermal variation of the stator resistance especially at low speed, parallel speed and stator resistance estimation scheme has been used to estimate the rotor speed and eliminate the effect of stator resistance. Measurements of two stator phase voltages and currents are transformed to d^s - and q^s – components and used in the adaptive rotor resistance and speed. The coordinate transformation (CT) in Fig. 4-3 is used to transform the stator currents components command ($i_{qs}^{*\,e}$ and $i_{ds}^{*\,e}$) to the three phase stator current command (i_{as}^*, i_{bs}^* and i_{cs}^*) by using the field angle θ_e^*. The hysteresis current controller compares the stator current to the actual currents of the machine and switches the inverter transistors in such a way that commanded currents are obtained.

VI. Simulation Results and Discussion

The induction motor under study is a 3.8 HP, four poles motor, its nominal parameters and specifications are listed in table 1. The Matlab / Simulink software package has been used for evaluating the parallel MRAS estimator for rotor resistance and speed.

The performance of the sensorless indirect vector control of induction motor has been tested at the rated value of stator resistance. Fig.4 shows the simulation results when the actual stator resistance at the rated reference speed equal to 150 rad/sec. This figure shows that, with the stator resistance equal its nominal value in MRAS speed estimator, no error between the actual and estimated speeds has been indicated. The d-q axis rotor flux is kept equal to its command value. This mean the conditions of the indirect vector control is satisfied.

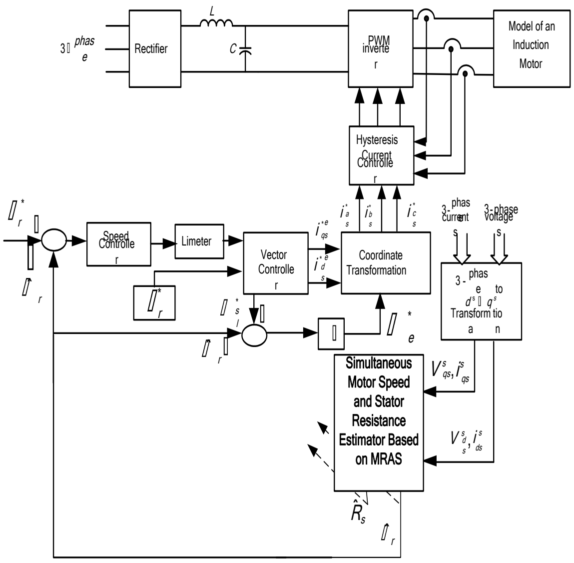

Fig.3: Block diagram of the proposed sensorless indirect vector controlled induction motor

Rated power (HP)	3.8	Rated voltage (V)	380
Rated current (A)	8	Rated frequency (Hz)	50
R_r (Ω)	1.009	R_s (Ω)	1.725
L_r (H)	0.1473	L_s (H)	0.1473
L_m (H)	0.1271	Rated rotor flux, (wb)	0.735
J (kg.m^2)	0.0400	Rated speed (rpm)	1450

Table 1: Parameters and data specifications of the induction motor

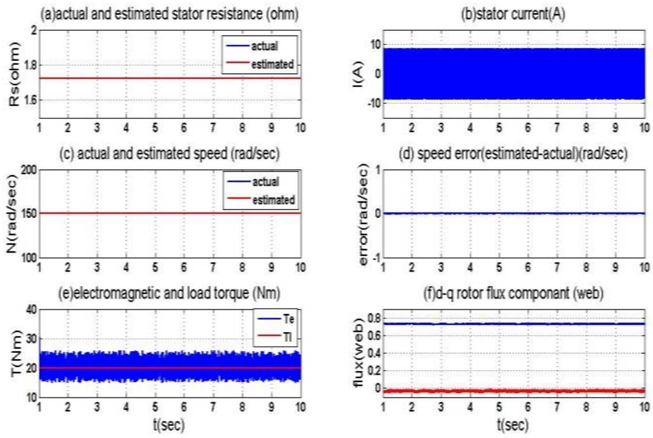

Fig. 4: Performance of the proposed sensorless drive system for Rs and Wr estimation at nominal parameter of the induction motor

The transient performance of the sensorless drive system is investigated for step change of the stator resistance when the motor is running at very low speeds of 10 r/s with nominal load torque. Fig.5a, b, c, d, e and f show the vector control response when the stator resistance is increased by 50 % from its nominal value at t = 5 sec. From figu.5a, b, c, d, e and f, it seen that the estimated stator resistance, motor stator current , estimated speed , speed error, motor torque, and $d-q$ axes rotor flux components are deviating from their command values during the stator resistance variation. Also, the figure indicates that the actual and estimated speeds are aligned in spite of the stator resistance variation. In addition, the d-axis rotor flux is kept equal to its command value even during the stator resistance variation. This mean the conditions of the indirect vector control is satisfied and good dynamic performance has been achieved. Figure 6, shows the simulation results at a speed of 150 rad/sec.

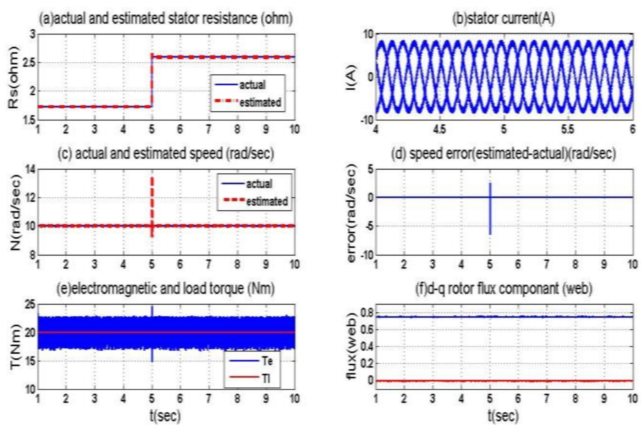

Fig.5: The dynamic Response of the drive system at variation of stator resistance by 50% at rotor speed of 10 rad/sec

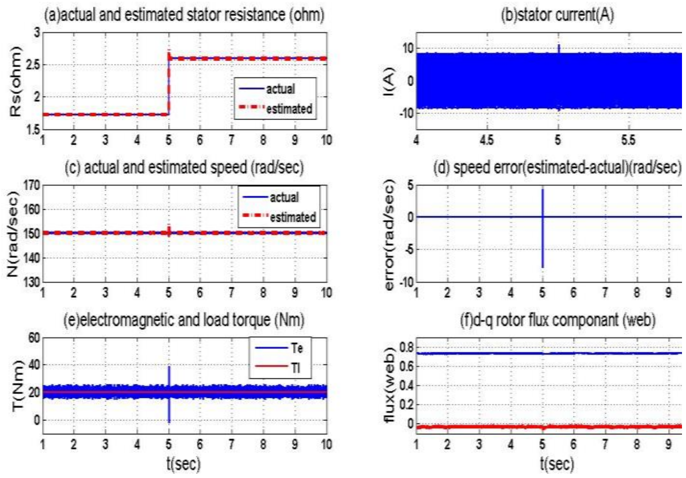

Fig.6: The dynamic Response of the drive system at variation of stator resistance by 50% at rotor speed of 150 rad/sec.

Also, a high dynamic performance has been achieved as shown figures. The figures with a good track of the estimated values of stator resistance and rotor speed with their actual values.

In order to validate the proposed scheme under load disturbance, the sensorless IM drive system has been tested with step change in the load torque from 10 N.m to 20 N.m. Fig.7 shows the vector control drive response when the stator resistance is increased by a 50 % of its nominal value with command speed equal to 10 r/s. This figure shows the actual and estimated stator resistance, stator current, actual and estimated speed of the proposed control system has been the same track, speed error, motor torque, and the d-axis rotor flux component equal to its command value. The figure, also, shows the q-axis rotor flux component is equal to zero that mean satisfying the vector control principles. Fig. 8, shows the simulation results at high speed of 150 rad/sec at the same conditions of fig.7.

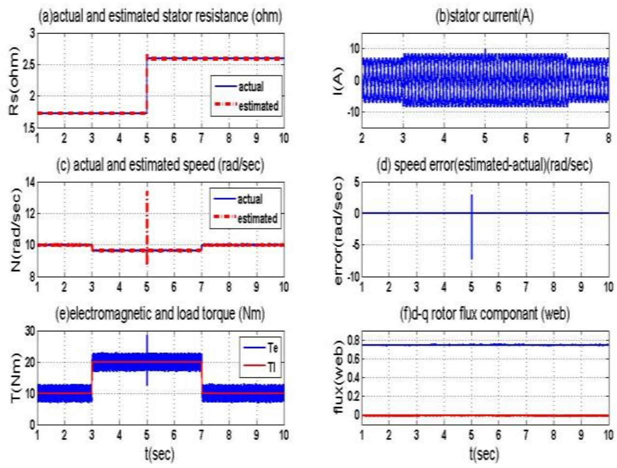

Fig.7: Performance of the proposed sensorless drive system for load torque disturbance and stator resistance variation by 50% step change at very low speed .

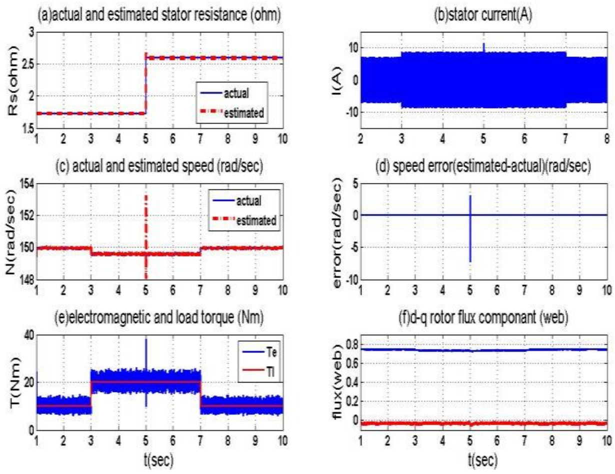

Fig.8: Performance of the proposed sensorless drive system for load torque disturbance and stator resistance variation by 50% step change at high speed.

In the practical operating conditions, the rate of change on temperature is very slow and so that it is the change of stator resistance. The simulation results presented in Fig.9 corresponds to his situations at 10 rad/sec (very low speed), where the stator resistance variation is only of a slow ramp change, and step change in the load torque from 10 N.m to 20 N.m. The figure shows the results of actual and estimated stator resistance, three phase stator current, actual and estimated speeds, speed error between the actual and estimated speeds, load and electromagnetic torque and d-q rotor flux components. From this figure, there is no error between the actual and estimated speed. Also the d-axis rotor flux is constant and equal to its command, which leads to satisfying the vector control conditions and good dynamic performance. Fig.10shows the simulation results at high speed of 150 rad/sec.

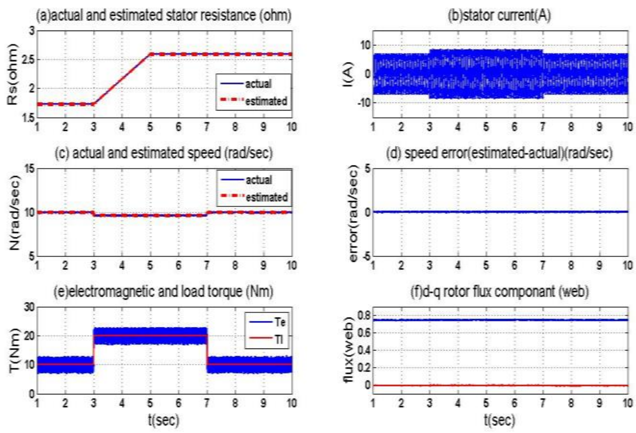

Fig.9: Performance of the drive with stator resistance estimations for 50% ramp change in stator resistance and load torque disturbance at very low speed.

In order to validate the effectiveness of the proposed sensorless drive with the proposed MRAS, the transient performance of the sensorless drive system is investigated with the multi-step of the rotor speed. Figure 11, 12, and 13 show the performance of the sensorless IM drive at different rotor speed 10, 100 and 150 rad/sec with a ramp change in the reference speed from the command speed to zero speed as shown in figures respectively with the ramp variation of rotor resistance and nominal load torque .

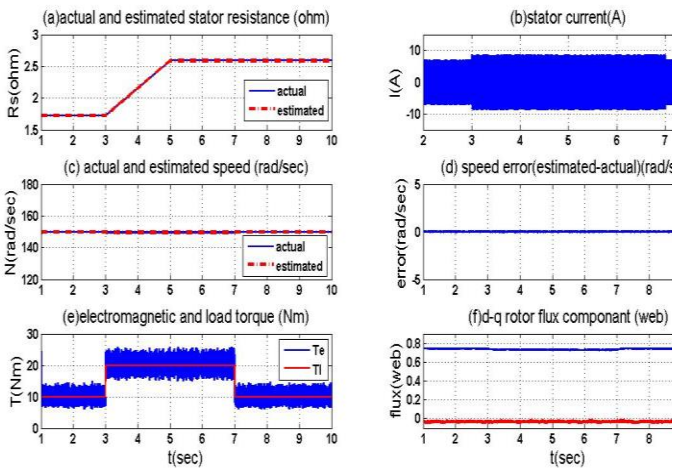

Fig.10: Performance of the drive with stator resistance estimations for 50% ramp change in stator resistance and load torque disturbance at high speed.

The figure shows the results of actual and estimated stator resistance, three phase stator current, actual and estimated speeds, speed error between the actual and estimated speeds, load and electromagnetic torque and d-q rotor flux components. From this figure, there is no error between the actual and estimated speed. Also the d-axis rotor flux is constant and equal to its command, which leads to satisfying the vector control conditions and good dynamic performance.

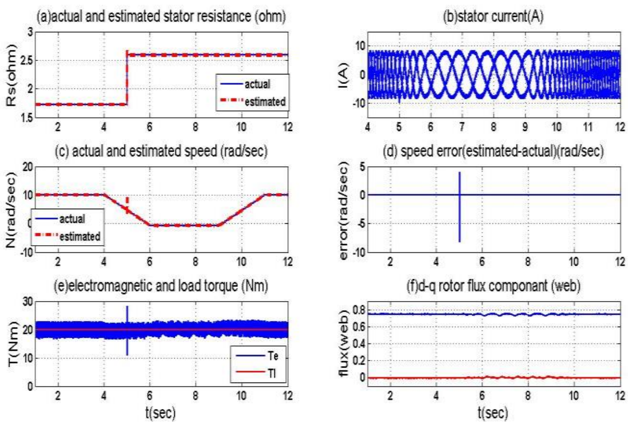

Fig.11: Performance of the proposed sensorless drive system at variation of the rotor speed and stator resistance at very low speed 10 rad/sec

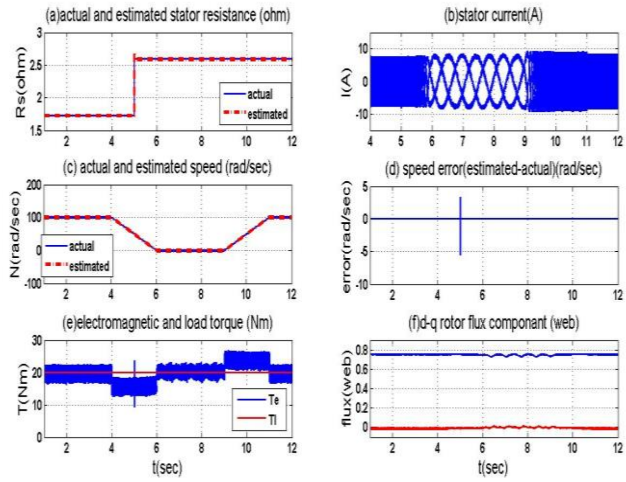

Fig.12: Performance of the proposed sensorless drive system at variation of the rotor speed and stator resistance at speed of 100 rad/sec.

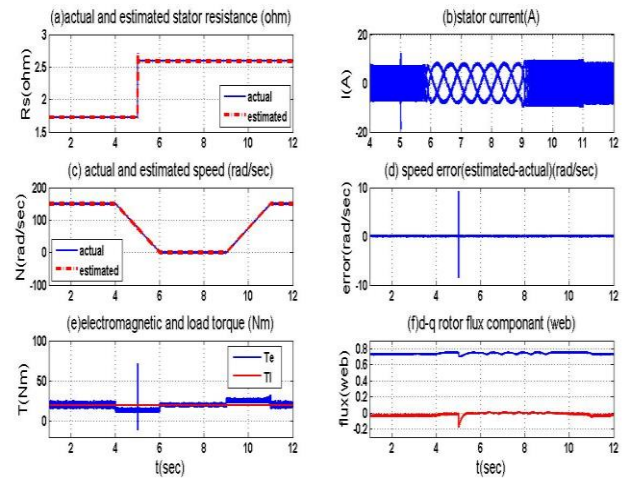

Fig.13: Performance of the proposed sensorless drive system at variation of the rotor speed and stator resistance at speed of 150 rad/sec

Conclusion

A novel speed sensorless IM drive is presented in this paper. The speed is controlled based on indirect vector control technique. The speed information are required for speed control. Also an accurate value of the stator resistance is required for high dynamic performance of indirect vector control drive. A novel MRAS is proposed for simultaneous estimation of stator resistance and rotor speed in parallel. The proposed MRAS is designed based of Popov's criterion to assure the stability of the IM sensorless drive. Simulation works are carried out to evaluate the proposed scheme performance at different operating conditions. The proposed scheme performance is satisfactory at very low speed as well as high speed operation. The estimated speed and stator resistance can trace well the actual speed and stator resistance, although, load disturbance.

References

[1] M. S. Zaky, M. M. Khater, H. Yasin, and S. S. Shokralla, A. El-Sabbe, "Speed-sensorless

control of induction motor drives (Review Paper)", Engineering Research Journal (ERJ), Faculty of Engineering, Minoufiya University, Egypt, Vol. 30, No. 4, October 2007, PP. 433-444.

[2] A. Consoli, G. Scarcella, and A.Testa," Slip-Frequency Detection for Indirect Field Oriented Control Drives".IEEETrans.Ind.Applic.,40 (1) (2004), pp. 194-201.

[3] C. Schauder, ―Adaptive speed identification for vector control of induction motors without rotational transducers,‖ IEEE Trans. Ind. Applicat., vol. 28, Sept. /Oct. 1992, pp. 1054–1061.

[4] H.A.Toliyat, E.Levi, M.Raina; "A review of RFO induction motor parameter estimation techniques", IEEE Trans. on Energy Conversion, vol. 18, no. 2, 2003, pp. 271-283.

[5] Yehia S. Mohamed, A. M. El-Sawy and A. A. Zaki ―Stator resistance Estimation for Speed Sensorless Vector Controlled InductionMotor Drives Taking Saturation into Account‖, Journal of Engineering Science, Assiut University, Vol. 37, May 2009, pp. 669-690.

[6] M. S. Zaky, M. M. Khater, H. Yasin, and S. S. Shokralla,A. El-Sabbe,"Speed-sensorless control of induction motor drives (Review Paper)", Engineering Research Journal (ERJ), Faculty of Engineering,Minoufiya University, Egypt, Vol. 30, No. 4, October 2007, PP. 433-444.

[7] Peng, Z.; Fukao, T.; "Robust speed identification for speed sensorless vector control of induction motors". IEEE Trans. on Ind. Appl. Vol. 30, no. 5, 1994, pp. 1234-1240.

[8] V. Vasic, S. N. Vukosavic, and E. Levi, "A Stator Resistance Estimation Scheme for Speed Sensorless Rotor Flux Oriented Induction Motor Drives". IEEE Trans. on Energy Conv., Vol. 18, NO. 4, December 2003, PP. 476-483.